Available online at www.sciencedirect.com
ScienceDirect
Ceramics International 35 (2009) 2927–2931
CERAMICS INTERNATIONAL
www.elsevier.com/locate/ceramint

Fabrication and properties of highly transparent $Tm_3Al_5O_{12}$ (TmAG) ceramics

Wen-Xin Zhang [a,b], Jiang Li [a], Wen-Bin Liu [a], Yu-Bai Pan [a,*], Jing-Kun Guo [a]

[a] *Key Laboratory of Transparent and Opto-functional Advanced Inorganic Materials, Shanghai Institute of Ceramics, Chinese Academy of Sciences, 1295 Ding Xi Road, Shanghai 200050, PR China*
[b] *Graduate School of the Chinese Academy of Sciences, 19A Yuquan Road, Beijing 100039, PR China*

Received 19 February 2009; received in revised form 4 March 2009; accepted 30 March 2009
Available online 24 April 2009

Abstract

Highly transparent $Tm_3Al_5O_{12}$ (TmAG) ceramics were fabricated by solid-state reaction and vacuum sintering. Densification, microstructure evolution, mechanical, thermal, and optical properties of the TmAG ceramics were investigated. Fully dense TmAG ceramic with average grain size of ~15 μm was obtained by sintering at 1780 °C for 20 h. The in-line transmittance was 80.5% at 2000 nm. The absorption coefficients at 682 nm and 785 nm were 8.03 cm^{-1} and 8.33 cm^{-1}, respectively. The Vickers hardness, the Young modulus, the bending strength, and the fracture toughness values were 15.14 GPa, 343 GPa, 230 MPa, and 2.35 MPa $m^{1/2}$, respectively. The thermal conductivity at room temperature was 3.3 W/m K and the average linear thermal expansion coefficient from 20 °C to 1000 °C was 8.915×10^{-6} K.

Keywords: C. Mechanical properties; C. Optical properties; C. Thermal properties; Transparent ceramic

1. Introduction

Thulium aluminum (TmAG) belongs to the crystal family of the rare-earth aluminum garnets ($RE_3Al_5O_{12}$, RE = rare-earth or yttrium). They are synthetic insulators and technologically play an important role as host crystals for near-infrared solid-state lasers. For example, yttrium aluminum garnet (YAG, $Y_3Al_5O_{12}$) is a well established laser host material due to its attractive thermal and optical properties [1,2].

TmAG has seven strong absorption bands. The central wavelengths are 262 nm, 357 nm, 460 nm, 682 nm, 785 nm, 1172 nm, and 1622 nm, respectively. They are produced by the transition of Tm^{3+} from the $^3H_6$ state to the $^3P_2$, $^1D_2$, $^1G_4$, $^3F_3$, $^3H_4$, $^3H_5$, and $^3F_4$ state, respectively [3]. Two absorption peaks located at 680 nm ($^3H_6 \rightarrow {}^3F_3$) and 785 nm ($^3H_6 \rightarrow {}^3H_4$) are the strongest, which are consistent with the emission wavelength of infrared diode and near-infrared diode. Therefore, TmAG could be a kind of excellent diode pumped laser medium [4].

Since Ikesue et al. fabricated highly transparent Nd:YAG ceramics and obtained laser output in 1995 [5], polycrystalline ceramic laser materials have attracted much attention because the optical quality has been improved greatly and highly efficient laser output can be obtained whose efficiencies are comparable or superior to those of single crystals [6,7]. Since then, many new laser ceramic material systems were developed in rapid succession. For example, Nd:LuAG [8], Nd:Y_2O_3 [9], Yb:Sc_2O_3 [10], Yb:$Y_3ScAl_4O_{12}$ [11], etc. However, TmAG transparent ceramics have not been developed yet.

In the present work, TmAG ceramics were fabricated by solid-state reaction and vacuum sintering using high-purity α-Al_2O_3 and Tm_2O_3 as raw materials with tetraethyl orthosilicate (TEOS) as a sintering aid. Densification, microstructure evolution, mechanical, thermal and optical properties of the TmAG ceramics were mainly studied in this paper.

2. Experimental procedure

High-purity α-Al_2O_3 (Shanghai Wusong Chemical Co. Ltd., 99.99%) and Tm_2O_3 (Conghua Jianfeng Rare-Earth Co. Ltd., 99.99%) were used as starting materials, which were both commercially available powders. These powders were blended

* Corresponding author. Tel.: +86 21 52412820; fax: +86 21 52413903.
E-mail address: ybpan@mail.sic.ac.cn (Y.-B. Pan).

0272-8842/$36.00 © 2009 Published by Elsevier Ltd and Techna Group S.r.l.
doi:10.1016/j.ceramint.2009.03.039

with the stoichiometric ratio of $Tm_3Al_5O_{12}$ and ball-milled with high-purity corundum balls for 12 h in ethanol, with a binder and addition of 0.5 wt% TEOS as a sintering aid. Then, the alcohol solvent was removed by drying the milled slurry at 80 °C for 4 h in oven. The dried powder mixture was ground and sieved through 200 mesh screen. After removing the organic component by calcining at 400–800 °C for 2 h, the powder mixture was pressed with low pressure into Φ25 mm and Φ60 mm disks in a steel mold and then cold-isostatic-pressed at 250 MPa. Then the specimens were vacuum-sintered at different temperatures for 20 h. After sintering, the specimens were annealed at 1450 °C for 10 h in air.

The phase composition of the specimen was identified by X-ray diffraction (Model D/MAX-2550V, Rigaku, Japan). Sintered density was measured by the Archimedes method, using deionized water as the immersion medium. Microstructures of the fracture and the mirror-polished surfaces of the samples were observed by electron microprobe analysis (EPMA, Model JXA-8100, JEOL, Japan).

Mirror-polished samples on both surfaces were used to measure optical transmittance and absorption spectra (Model U-2800 Spectrophotometer, Hitachi, Tokyo, Japan).

The sintered samples were machined into bars of $3 \times 4 \times 36$ mm^3 after being ground and polished. The bending strength and fracture toughness of the sintered samples were measured at room temperature. The three-point bending test was done in a universal testing machine (Model Instron-1195, INSTRON, Canton, USA) with a span of 30 mm between the supports and a crosshead speed of 0.5 mm min^{-1}. The bending strength for each batch was taken as the average of the strength of the three samples. Fracture toughness values (KIC) were determined by crack indentation technique in a materials testing machine (Model Instron Wilson-Wolpert-Tukon 2100B, INSTRON, Canton, USA) under load of 50 N. The fracture toughness for samples was taken as the average value of three data points.

The specific heat (C_p) of the sample (Φ5.5 mm × 0.5 mm) was measured by a differential scanning calorimeter (DSC, Model DSC-2C, Perkin Elmer, Norwalk, USA) at room temperature. The thermal diffusivity (α) of the sample (Φ10.0 mm × 2.0 mm) was measured by a laser flash method by means of a thermal constant analyzer developed by our institute. The thermal conductivity (κ) was calculated from the equation below:

$$\kappa = \alpha \rho C_p$$

where ρ is the density. Linear coefficient of thermal expansion was measured from 20 °C to 1000 °C at a heating rate of 5 °C/min using a dilatometer (Model DIL 402C, Netzsch, Selb, Germany), and the dimension of the sample was $5 \times 5 \times 25$ mm^3.

3. Results and discussion

Fig. 1 shows the XRD patterns of the samples sintered between 1650 °C and 1780 °C for 20 h. All the diffraction peaks can be well indexed as the cubic garnet structure of $Tm_3Al_5O_{12}$ (TmAG, JCPDS 17-0734). At 1650 °C, TmAG phase forms and all the characteristic peaks of TmAG phase appear, but still some other phase exists. When the sintering temperature goes up to 1700 °C, there are no other phases detected. With further increase in the sintering temperature to 1780 °C, the diffraction peaks of crystalline TmAG become much sharper and stronger, indicating that crystallinity has been almost fully achieved.

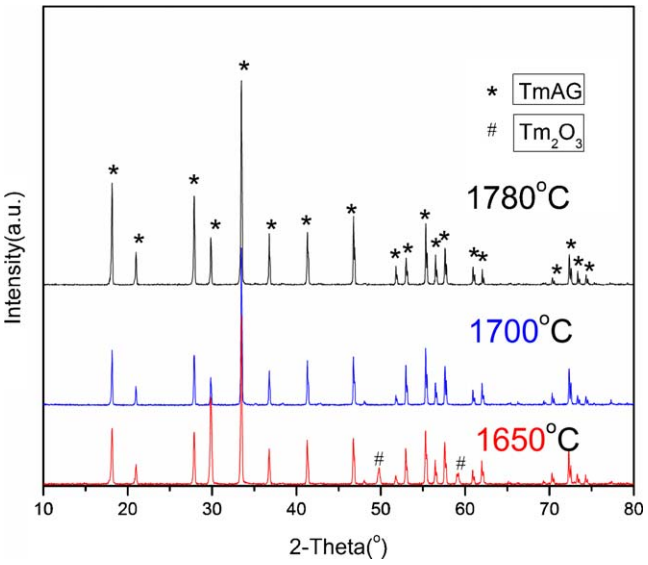

Fig. 1. XRD patterns of the samples sintered between 1650 °C and 1780 °C for 20 h.

Fig. 2 shows the relative density of the vacuum-sintered TmAG specimens as a function of sintering temperature. It can be seen that densification occurred mainly from 1550 °C to 1750 °C. At the temperature range of 1550–1750 °C, the increase of temperature distinctly enhances densification and the relative density increases from 61.5% of the theoretical value (6.4 g/cm^3) to 99.7%. With further increase of temperature, the density remains almost unchanged.

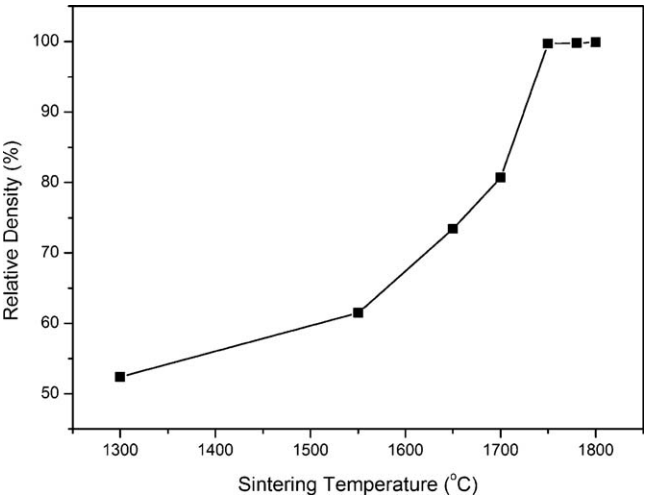

Fig. 2. Relative density of the vacuum-sintered TmAG specimens as a function of sintering temperature.

Table 1
Mechanical property values for TmAG ceramic and YAG ceramic.

Mechanical property	TmAG ceramic	YAG ceramic
Young modulus (GPa)	343	221
Vickers hardness (GPa)	15.14	12.5
Fracture toughness (MPa $m^{1/2}$)	2.35	2.21
Bending strength (MPa)	230	229

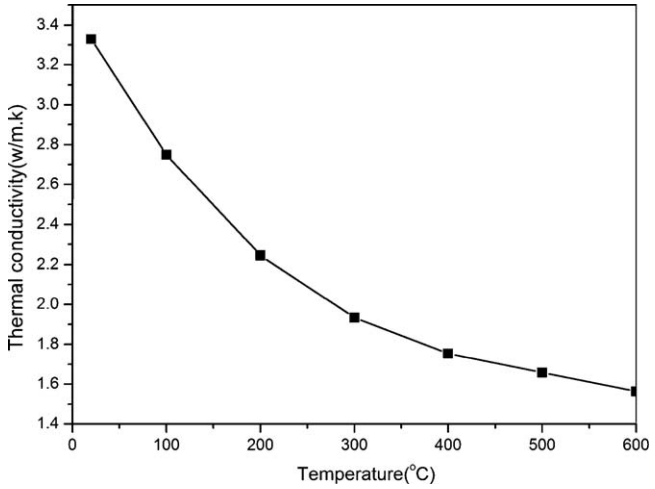

Fig. 3. The thermal conductivity values of TmAG ceramic as a function of temperature.

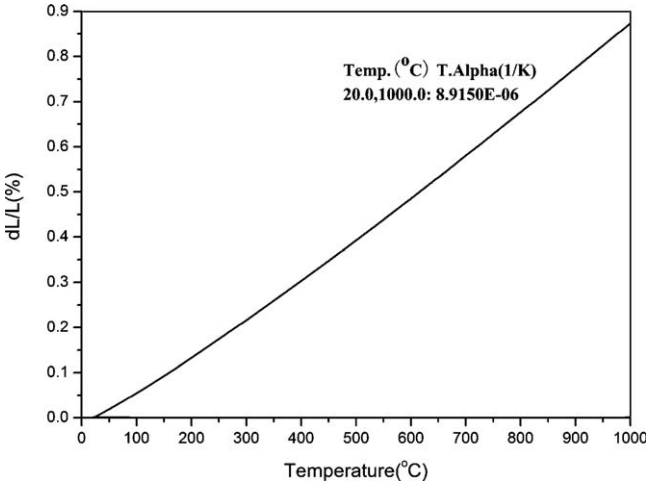

Fig. 4. The thermal expansion values of TmAG ceramic as a function of temperature.

Table 1 contrasts the mechanical property values for TmAG ceramic obtained in the current study and those of YAG ceramic from the literature [12]. It can be seen that the mechanical properties of the prepared TmAG ceramic are very similar or superior to those of YAG ceramic, and indicating its mechanical reliability during the operation.

Fig. 3 shows the thermal conductivity values of TmAG ceramic as a function of temperature. The thermal conductivity at room temperature was 3.3 W/m K. The thermal conductivity

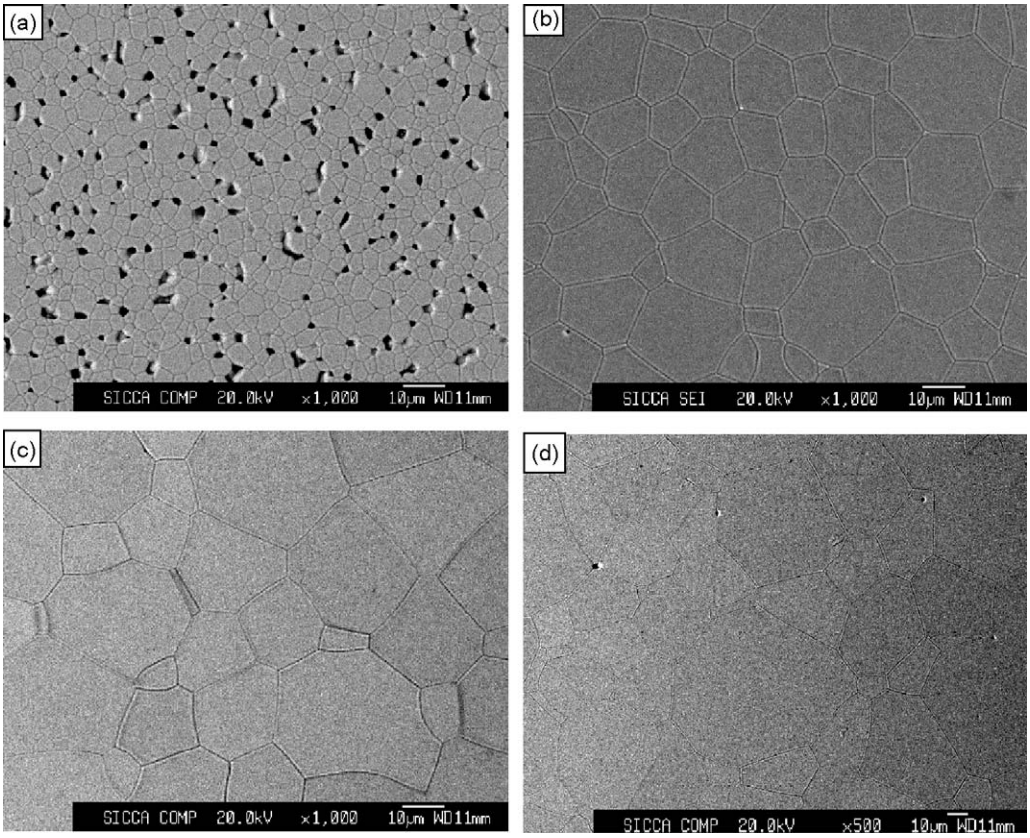

Fig. 5. EPMA micrographs of the mirror-polished and thermal-etched surfaces of the TmAG ceramics (thermal-etched at 1500 °C for 1 h) sintered at: (a) 1700 °C; (b) 1750 °C; (c) 1780 °C; (d) 1800 °C for 20 h.

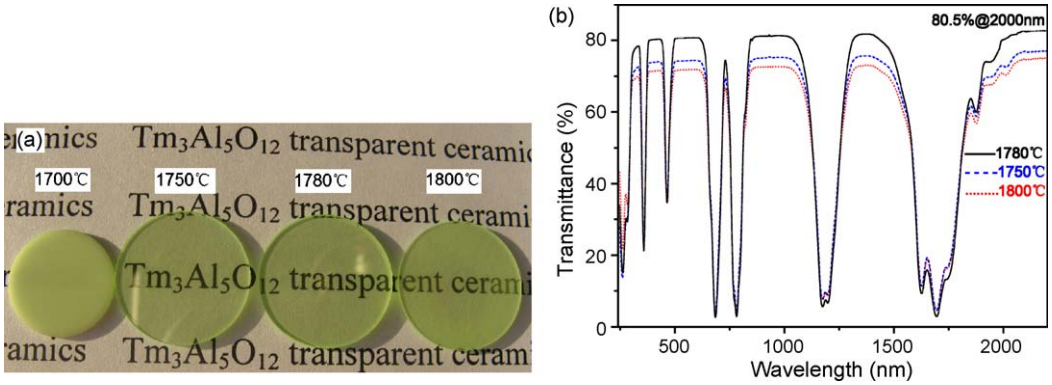

Fig. 6. Appearance (a) and optical transmission spectra (b) of TmAG ceramics sintered at different temperatures for 20 h.

of TmAG ceramic decreased with increase of temperature, mainly due to the decrease of phonon mean free path.

Fig. 4 shows the thermal expansion values of TmAG ceramic as a function of temperature. It could be seen that the thermal expansion curve was essentially linear increase in the temperature of 20–1000 °C. The average linear thermal expansion coefficient from 20 °C to 1000 °C was 8.915 $\times 10^{-6}$ K.

Fig. 5 shows the EPMA micrographs of the mirror-polished and thermal-etched surfaces of the TmAG ceramics sintered at 1700–1800 °C for 20 h. It can be seen that the grain size increases and the pore decreases with the increase of sintering temperature. For the sample sintered at 1700 °C, quite a few pores are captured in the grain boundaries and the average grain size is about 4 μm. The residual pores are gradually removed with the increase of sintering temperature. A dense and pore-free microstructure is observed at 1780 °C and the average grain size is about 15 μm. Obvious grain growth occurs between 1700 °C and 1750 °C and grain size increases from 4 μm to 10 μm. Abnormal grain growth is not observed for the sample sintered at 1780 °C or below. In our study, it appears that grain growth is an important process to remove the final large pores and to obtain TmAG transparent ceramics, as reported by Kingery and Francois [13], and by Slamovich and Lange [14]. With further increase in the sintering temperature to 1800 °C, some abnormal grain growth is observed, and several pores enveloped in the abnormal grains will be the scattering centers, which can significantly reduce the optical transmittance of the specimen.

Fig. 6(a) shows appearance of the mirror-polished specimens (1 mm thick) sintered at 1700 °C, 1750 °C, 1780 °C, and 1800 °C for 20 h. The specimen sintered at 1700 °C is opaque because of its higher porosity. The specimens sintered at 1750 °C and 1800 °C are cloudy, whereas the specimen sintered at 1780 °C is fully transparent, as shown in Fig. 6(a).

Fig. 6(b) shows the optical transmission spectra of TmAG ceramics (sintered at 1750 °C, 1780 °C, and 1800 °C for 20 h) in the wavelength ranging from 240 nm to 2200 nm, respectively. It is consistent with the result of the EPMA. The specimen sintered at 1780 °C is of the highest transmittance, whose in-line transmittance reaches 80.5% at 2000 nm. While the specimen sintered at 1800 °C is of the lowest transmittance, due to the pores enveloped in the abnormal grains.

Fig. 7 shows the absorption spectrum of TmAG ceramic sintered at 1780 °C for 20 h. The absorption coefficients at 682 nm and 785 nm were 8.03 cm^{-1} and 8.33 cm^{-1}, respectively.

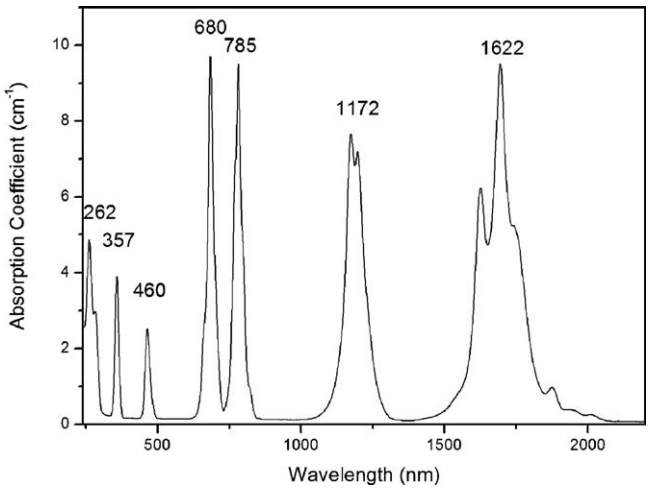

Fig. 7. Absorption spectrum of TmAG ceramic sintered at 1780 °C for 20 h.

4. Conclusions

Dense TmAG transparent ceramics were fabricated successfully by the solid-state reaction method and vacuum sintering. For the TmAG ceramic sintered at 1780 °C for 20 h, the main results can be summarized as follows:

(1) The average grain size of the dense TmAG ceramic was about 15 μm. Pores and secondary phase were not observed.
(2) The in-line transmittance was 80.5% at 2000 nm. The absorption coefficients at 682 nm and 785 nm were 8.03 cm^{-1} and 8.33 cm^{-1}, respectively.
(3) The Vickers hardness, the Young modulus, the bending strength, and the fracture toughness values were 15.14 GPa, 343 GPa, 230 MPa, and 2.35 MPa $m^{1/2}$, respectively. Overall, the mechanical properties of the prepared TmAG ceramics were very similar or superior to those of YAG ceramic.

(4) The thermal conductivity at room temperature was 3.3 W/m K and the average linear thermal expansion coefficient from 20 °C to 1000 °C was 8.915×10^{-6} K.

Acknowledgments

The authors are very grateful for the financial supports from the 863 project (no. AA03Z523) and the Major Basic Research Programs of Shanghai (no. 07DJ14001).

References

[1] K. Papagelis, G. Kanellis, T. Zorba, S. Ves, G.A. Kourouklis, Infrared lattice spectra of $Tm_3Al_5O_{12}$ and $Yb_3Al_5O_{12}$ single crystals, J. Phys.: Condens. Matter 14 (4) (2002) 915–923.

[2] Y.S. Wu, J. Li, Y.B. Pan, Q. Liu, J.K. Guo, B.X. Jiang, J. Xu, Diode pumped Yb:YAG ceramic laser, J. Am. Ceram. Soc. 90 (10) (2007) 3334–3337.

[3] C.T. Wu, Y.L. Ju, Z.G. Wang, Q. Wang, C.W. Song, Y.Z. Wang, Diode-pumped single frequency Tm:YAG laser at room temperature, Laser Phys. Lett. 5 (11) (2008) 793–796.

[4] A. Ikesue, T. Kinoshita, K. Kamata, K. Yoshida, Fabrication and optical properties of high-performance polycrystalline Nd:YAG ceramics for solid-state lasers, J. Am. Ceram. Soc. 78 (4) (1995) 1033–1040.

[5] A. Ikesue, I. Furusato, K. Kamata, Fabrication of polycrystalline, transparent YAG ceramics by a solid-state reaction method, J. Am. Ceram. Soc. 78 (1) (1995) 225–228.

[6] I. Shoji, S. Kurimura, Y. Sato, T. Taira, Optical properties and laser characteristics of highly Nd^{3+}-doped $Y_3Al_5O_{12}$ ceramics, Appl. Phys. Lett. 77 (7) (2000) 939–941.

[7] J. Lu, M. Prahu, J. Xu, K. Ueda, H. Yagi, T. Yanagitani, A.A. Kaminskii, Highly efficient 2% Nd:yttrium aluminum garnet ceramic laser, Appl. Phys. Lett. 77 (23) (2000) 3707–3709.

[8] J. Lu, K. Takaichi, T. Uematsu, A. Shirakawa, M. Musha, K. Ueda, H. Yagi, T. Yanagitani, A.A. Kaminskii, Highly transparent Nd^{3+}:Lu_2O_3 ceramic, Appl. Phys. Lett. 81 (23) (2002) 4324–4326.

[9] J. Lu, T. Murai, K. Takaichi, T. Uematsu, K. Ueda, H. Yagi, T. Yanagitani, A.A. Kaminskii, Nd^{3+}:Y_2O_3 ceramic laser, Jpn. J. Appl. Phys. 40 (12A) (2001) L1277–1279.

[10] J. Lu, J.F. Bisson, K. Takaichi, T. Uematsu, A. Shirakawa, M. Musha, K. Ueda, H. Yagi, T. Yanagitani, A.A. Kaminskii, Yb^{3+}:Sc_2O_3 ceramic laser, Appl. Phys. Lett. 83 (6) (2003) 1101–1103.

[11] J. Saikawa, Y. Sato, T. Taira, A. Ikesue, Passive mode locking of a mixed garnet Yb:$Y_3ScAl_4O_{12}$ ceramic laser, Appl. Phys. Lett. 85 (11) (2004) 1898–1900.

[12] J. Li, Y.S. Wu, Y.B. Pan, Fabrication, microstructure and properties of highly transparent Nd:YAG laser ceramics, Opt. Mater. 31 (1) (2008) 6–17.

[13] W.D. Kingery, B. Francois, Grain growth in porous compacts, J. Am. Ceram. Soc. 48 (10) (1965) 546–547.

[14] E.B. Slamovich, F.F. Lange, Densification of large pores. Part I. Experiments, J. Am. Ceram. Soc. 75 (9) (1992) 2498–2508.